J. Chem. Sci. (2021)133:91
https://doi.org/10.1007/s12039-021-01951-0

REGULAR ARTICLE

Special Issue on Beyond Classical Chemistry.

Thermotropic phase behavior and supramolecular organization of *N*,*O*-diacyl-L-alaninols: effect on stratum corneum model membrane

DOKKU SIVARAMAKRISHNA, SUMAN KUMAR CHOUDHURY and MUSTI J SWAMY*
School of Chemistry, University of Hyderabad, Hyderabad 500 046, India
E-mail: mjswamy@uohyd.ac.in; mjswamy1@gmail.com

MS received 15 April 2021; revised 3 June 2021; accepted 8 June 2021

Abstract. In recent years, chemical enhancers that increase the permeability of stratum corneum (SC) attracted the attention of clinicians and researchers due to their utility in developing transdermal drug delivery systems. *N*-Lauroyl glycine lauryl ester (NLGLE) was reported to induce higher SC permeability than *N*-lauroyl serine lauryl ester (NLSLE). Earlier, we proposed a similar activity could be obtained by *N*-acyl-L-alanine esters (NAAEs) towards SC, which are homologous to NLGLE. In this study, we synthesized a homologous series of *N*,*O*-diacyl-L-alaninols (DAAOHs) (which are isomers of NAAEs) with saturated acyl chains. We investigated their thermotropic phase behavior and supramolecular organization, and the results are discussed with the properties of isomeric NAAEs. Most DAAOHs exhibited one polymorphic phase transition (solid-solid transition) before the melting transition in the first heating thermogram. The solid-solid transition disappeared in further heating thermograms. Odd chainlength DAAOHs exhibited higher transition enthalpy and transition entropy values than even chainlength DAAOHs. Interestingly, the even chainlength DAAOHs exhibited higher transition temperature and *d*-spacing values than odd chainlength DAAOHs. Further, Laurdan fluorescence studies revealed that *N*,*O*-dilauroyl-L-alaninol increases the fluidity of SC model membrane more efficiently as compared to NLGLE, suggesting that DAAOHs can potentially be used as chemical enhancers in developing transdermal drug delivery systems.

Keywords. *N*,*O*-diacyl alaninols; stratum corneum; Differential scanning calorimetry; powder X-ray diffraction; Laurdan fluorescence; generalized polarization; membrane fluidity.

1. Introduction

Transdermal drug delivery (TDD) is a convenient and safe approach compared to conventional drug delivery methods of subcutaneous/intravenous injection, and oral administration. TDD avoids the hepatic first-pass effect, especially for drugs with low bioavailability through conventional administration, and when high doses of medication are necessary for a longer duration to get effective bioavailability.[1] Several anti-dermal, anti-ischemic, anti-hypertensive and hypoglycemic drugs, as well as some others are widely delivered in a transdermal form.[1,2] However, due to the low permeability of drugs through the stratum corneum (SC), the use of TDD is considerably restricted. SC or epidermis is the outer layer of skin, which serves as the primary barrier between the environment and the body. SC consists of dead cells (Corneocytes) without nuclei and cell organelles and contains cytoplasm with filamentous keratin. The major lipid components of the SC are ceramides (40-60%), sterols (20-33%), and fatty acids (7-13%), whereas cholesterol-3-sulphate and cholesteryl esters are minor components.[3–5] However, the lipid composition varies based on a variety of parameters, e.g., location (depth of the skin), age, sex, race, and health of the individual. The ceramides in SC are complex and contain primarily saturated fatty acids, due to which permeability of drugs through SC is rather low.[4,6]

*For correspondence

Supplementary Information: The online version contains supplementary material available at https://doi.org/10.1007/s12039-021-01951-0.

Published online: 03 September 2021

Several chemical enhancers (CEs) have been investigated with the objective of improving the permeability of SC to drugs and therapeutic agents. These CEs include short and long-chain alcohols, propylene glycol and its esters, benzoic acid esters, fatty acid esters, cyclic amides, unsaturated fatty acids, etc. However, the exact mechanism of how CEs enhance SC's permeability is not well understood. It is assumed that most CEs enhance the permeability by changing the SC lipid organization and protein hydration by their bent structure, hydration capabilities and partition differences.[7–9] Earlier, *N*-acyl glycine alkyl esters (NAGEs) and *N*-acyl serine alkyl esters (NASEs), which are structurally similar to ceramides, have been reported to enhance the permeability of SC. NAGEs have shown a significant enhancement of permeability as compared to NASEs. The reduced/low ability of NASEs has been explained as due to the higher hydrophilic nature of the head group, which improves hydrogen bonding between adjacent lipid molecules, which results in improved resistance to the passage of the drug through SC.[10] In previous work, we synthesized and characterized *N*-acyl-L-alanine alkyl esters (NAAEs), which are homologous to NAGEs and hydrophobic analogs of NASEs, and proposed them as potential CEs for enhancing the permeability of SC given their reduced hydrogen bonding capacity.[11] With the objective of identifying other CEs for application in TDD, in the present study we synthesized and characterized a homologous series of *N*, *O*-diacyl-L-alaninols (DAAOHs) (see Figure 1 for the structures of the above classes of compounds). The ability of these 4 classes of compounds to modulate the fluidity of stratum corneum model membrane (SCM) was investigated by monitoring Laurdan fluorescence properties, considering that membrane fluidity provides a good correlation to membrane permeability.[12] The results obtained have been presented here and their potential for use in developing transdermal drug delivery systems has been discussed.

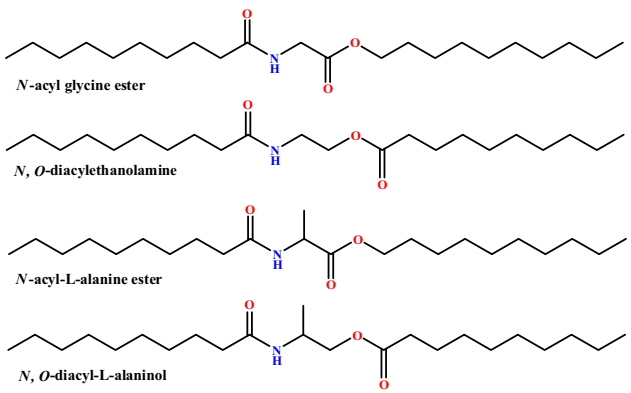

Figure 1. Molecular structure of *N*-acyl glycine ester (NAGE), *N, O*-diacylethanolamine (DAE), *N*-acyl-L-alanine ester (NAAE), and *N, O*-diacyl-L-alaninol (DAAOH) with matched acyl-alkyl/acyl-acyl chains.

The above introduction indicates that *N*-acyl amino acid esters are a new class of compounds that may find use as CEs in formulating TDD systems. Recent studies on the structure and supramolecular organization of NAGEs revealed that these amphiphilic molecules are packed in an untitled, normal bilayer mode.[13] This raised a question as to how the untilted NAGEs improve the permeability of the tightly packed SC lipid membrane. Further, how do the *N*, *O*-diacylethanolamines (DAEs), which adopt a bent structure,[14] influence the SC permeability? Additionally, how do isomeric NAAEs and DAAOHs differ from one another with respect to modulating SC permeability? How do isomeric NAGEs and DAEs, and homologous NAAEs and DAAOHs show their impact on SCM? We attempt to address these questions in the present study.

2. Materials and methods

2.1 *Materials*

Fatty acids (C9-C18) and L-alaninol were obtained from Sigma-Aldrich (Bangalore, India). Oxalyl chloride was purchased from Merck (Germany), and the remaining chemicals and solvents were obtained from Sisco Research Laboratories (Mumbai, India).

2.2 *Synthesis of DAAOHs*

DAAOHs of matched acyl chains were synthesized by a two-step procedure (Scheme 1). In the first step, *N*-acyl-L-alaninols (NAAOHs) were prepared as described earlier.[15] In the second step, the NAAOHs were *O*-acylated to yield DAAOHs. Briefly, the fatty acid (1 mmol) was converted to the acid chloride by mixing with oxalyl chloride (4 mmol) in dichloromethane (DCM) under a dry N_2 atmosphere. After two hours, excess oxalyl chloride was removed by passing dry N_2 gas. The acid chloride thus obtained was added to L-alaninol (4 mmol) in DCM at low temperature (0-5 °C), and the mixture was kept under stirring for 3 h. The crude NAAOH obtained after removing the excess DCM was then *O*-acylated as follows. Acid chloride of matched acyl chain length, prepared as mentioned above (1.1 mmol), was added to NAAOH (1 mmol) in DCM at room temperature, and the

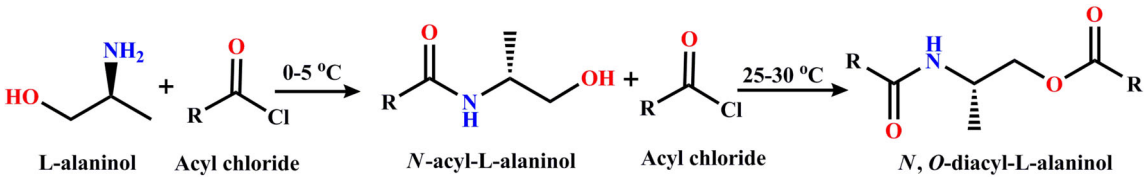

Scheme 1. Synthesis of *N*, *O*-diacyl-L-alaninols.

reaction mixture was kept under continuous stirring overnight. After removing excess solvent, the reaction mixture was washed with water and brine solution, which yielded the crude DAAOH. Crude DAAOHs thus obtained were purified by silica gel column chromatography. Ethyl acetate/n-hexane mixtures of varying ratios were used for elution. Finally, pure products were obtained in 70-80% yield after recrystallization from DCM containing trace amounts of acetone solvent at low temperature (ca. -20 °C). The purified DAAOHs were characterized using IR, NMR (^{1}H and ^{13}C), and high-resolution mass spectrometry (HRMS).

2.3 *Differential scanning calorimetry*

DSC experiments with dry DAAOHs were carried out on a Perkin Elmer Diamond differential scanning calorimeter as described earlier.[11] About 2 mg of each dry DAAOH was weighed accurately into an aluminum sample pan, covered with an aluminum lid and sealed with the aid of crimper. Another pan, prepared similarly but without any sample in it was used as the reference. For every sample, alternate heating (3) and cooling (2) scans were collected at a scan rate of 2 °C/min. Most of the compounds showed minor transitions in the first heating scan which disappeared in the subsequent heating scans; therefore, the first heating scans were considered for further analysis. Transition temperatures (T_t) were determined from the peak of the transition curve and transition enthalpies (ΔH_t) were determined by integrating the area under the transition curve, whereas transition entropies (ΔS_t) were obtained from the ΔH_t values assuming a first-order transition, indicated by Eq. (1):[16]

$$\Delta S_t = \Delta H_t / T_t \quad (1)$$

2.4 *Powder X-ray diffraction studies*

Powder X-ray diffraction measurements on DAAOHs were carried out using a Bruker SMART D8 Advance powder X-ray diffractometer (Bruker-AXS, Karlsruhe, Germany) with Cu-Kα radiation operating at 40 kV and 30 mA. Finely powdered samples were placed in the instrument sample holder and diffraction data were collected using a LynxEye PSD data collector over a 2θ range of 1–50° at room temperature with a step size of 0.0198° and a measuring time of 1.5 s for each step. Peaks corresponding to $2\theta \leq 20°$ were used to calculate d-spacings employing Bragg's equation.

2.5 *Stratum corneum model membrane preparation and Laurdan fluorescence*

Stratum corneum model membrane (SCM) was prepared from *N*–acetyl ceramide (C2-ceramide) (60 mol%), cholesterol (30 mol%), and palmitic acid (10 mol%). Twenty mol% of *N, O*-dilauroyl-L-alaninol (DLAOH), *N*-lauroyl-L-alanine lauryl ester (NLALE), *N, O*-dilauroylethanolamine (DLE), and *N*-lauroyl glycine lauryl ester (NLGLE) were added to the above lipid mixture in separate experiments to check their ability to modulate the fluidity of SCM. The final lipid composition in these samples was C2-ceramide (50 mol%), cholesterol (25 mol%), palmitic acid (8.3 mol%), DLAOH/DLE/NLGLE/NLALE (16.7 mol%). Stock solutions of C2-ceramide, cholesterol, palmitic acid, DLAOHs, NLALE, DLE, and NLGLE were prepared by dissolving in a mixture of chloroform and methanol (1:1, v/v). Samples with the above-mentioned lipid composition were obtained by mixing appropriate aliquots of the stock solutions of each lipid component. Similarly, a stock solution of the fluorescent dye Laurdan was prepared in ethanol, and an aliquot from it was added to the lipid mixture in chloroform-methanol to give a final probe concentration of 1 μM [1 mM lipid and 1 μM probe (1:1000 dilution)]. Then the solvent was evaporated by gently blowing dry nitrogen gas over the sample, and the remaining traces of solvent were removed by vacuum desiccation. Each sample was hydrated with 20 mM sodium phosphate buffer (pH 7.4) and subjected to 4-5 freeze-thaw cycles to get a homogeneous mixture. Laurdan fluorescence spectra were collected as reported earlier,[17] and generalized

polarization (GP) values were calculated using equation 2.[18]

$$GP = (I_{433} - I_{503})/(I_{433} + I_{503}) \quad (2)$$

where I_{433}, I_{503} are the emission intensities at 433 and 490 nm, respectively.

3. Results and Discussion

The homologous series of DAAOHs synthesized in the current study were characterized comprehensively by FTIR, ^{1}H- and ^{13}C-NMR spectroscopy and by high resolution mass spectrometry. Details of the spectral data and their analysis are given in Supporting Information (Tables S1-S4 and Figures S1-S4, Supplementary Information). These data are fully consistent with the structures of DAAOHs and show that they are all highly pure.

3.1 *Thermotropic phase behavior of DAAOHs*

Heating thermograms of dry DAAOHs bearing matched odd- and even acyl chains are given in Figure 2A and B, respectively, and the corresponding cooling thermograms are shown in Figure S5A (SI) and B. DAAOHs bearing different acyl chains (12-18 C-atoms) show two transitions, whereas those with 9-11 C-atoms show a single transition (Figure 2). The minor transitions most likely correspond to solid-solid phase transitions and suggest polymorphism in the solid-state structures of the compounds. The minor transition in even-chain DAAOHs are relatively less intense than those observed with odd-chain DAAOHs. The minor transition of C15 DAAOH is shifted towards a major transition compared to C13 DAAOH, whereas it is partially merged with a major transition in C17 DAAOH. It is interesting to note that minor transitions are not observed in the case of NAAEs and NAGEs (which are structural analogs and homologs of DAAOHs), while homologous DAEs showed minor transitions in the first heating thermograms.[11,13,14] *N*-Acyl derivatives of alanine and alaninol, namely *N*-acyl-L-alanines (NAAs) and *N*-acyl-L-alaninols (NAAOHs) also did not show any minor transitions, whereas even-chain ester derivatives of L-alanine (AEs) showed one minor transition in the first heating thermogram.[15,19,20]

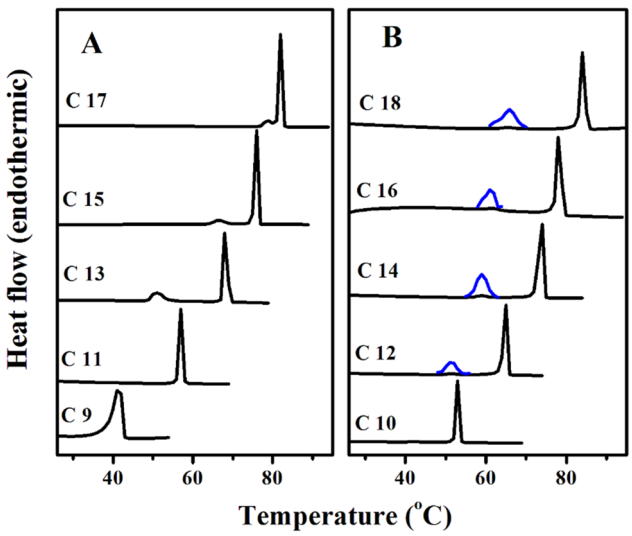

Figure 2. DSC first heating thermograms of dry DAAOHs with odd (A) and even (B) number of C-atoms in the acyl chain. The number of C-atoms is indicated against each thermogram. Less-intense minor transitions of even-chain DAAOHs are vertically expanded 15 times and shown in blue color.

The sharp transition temperatures of DAAOHs matched very well with the capillary melting points of the compounds. When the same samples were subjected to further heating scans, minor transitions for both even- and odd DAAOHs (C12-18) completely disappeared in the second and subsequent heating cycles and a slight decrease in the transition enthalpies was noticed in the second heating scans (Figure S6 (SI), Table 1). The minor transition were not seen in the first cooling scans also (Figure S5, SI). Similar behavior was noticed earlier in several single-chain and double-chain amphiphiles.[14,17,20–24] Interestingly, the minor transitions were also seen in the second heating scans in the case of *N*-acyl-β-alanines.[25] Values of T_t, ΔH_t, and ΔS_t of DAAOHs determined from the first and second heating thermograms are given in Table 1.

3.2 *Chainlength dependence of ΔH_t and ΔS_t*

The chainlength dependence of ΔH_t and ΔS_t corresponding to the phase transitions of DAAOHs in the first and second heating thermograms is shown in Figures 3A and B, and Figures S7A (SI) and B, respectively. In Figure 3, the ΔH_t and ΔS_t values of odd chainlength DAAOHs are somewhat higher as compared to the even chainlength compounds, except for the C10 compound. A similar pattern was observed earlier in NAAEs, which are structural isomers of DAAOHs. Besides, a similar pattern was noticed in the case of NAAs, while such pattern is missing in

Table 1. Average values of transition temperatures (T_t), transition enthalpies (H_t), and transition entropies (S_t) of DAAOHs from first and second heating thermograms. Values in parentheses correspond to standard deviations from three independent measurements.

	1st Heating			2nd Heating		
Acyl chain length (n)	T_t (°C)	ΔH_t (kcal mol^{-1})	ΔS_t (cal mol^{-1} K^{-1})	T_t (°C)	ΔH_t (kcal mol^{-1})	ΔS_t (cal mol^{-1} K^{-1})
9	41.8 (0.1)	7.55 (0.19)	24.0 (0.6)	41.8 (0.1)	7.55 (0.19)	24.0 (0.6)
10	53.2 (0.1)	10.39 (0.13)	31.8 (0.4)	53.1 (0.1)	10.31 (0.12)	31.6 (0.4)
11	57.4 (0.1)	12.17 (0.22)	36.8 (0.7)	56.9 (0.1)	11.39 (0.22)	34.5 (0.7)
12	64.8 (0.2)	13.28 (0.09)	39.3 (0.2)	64.7 (0.2)	13.19 (0.46)	39.1 (1.4)
13	68.4 (0.1)	18.37 (0.36)	53.7 (1.1)	67.6 (0.1)	14.64 (0.32)	43.0 (0.9)
14	73.5 (0.3)	17.43 (0.27)	50.3 (0.8)	73.3 (0.2)	16.29 (0.33)	47.0 (1.0)
15	76.0 (0.1)	22.17 (0.35)	63.5 (0.9)	75.3 (0.1)	17.65 (0.32)	50.7 (0.9)
16	79.4 (0.1)	20.64 (0.35)	58.5 (1.0)	78.9 (0.1)	19.55 (0.39)	55.5 (1.1)
17	82.5 (0.2)	26.91 (0.66)	75.8 (1.9)	81.8 (0.1)	21.09 (0.60)	59.2 (1.8)
18	84.8 (0.1)	24.06 (1.04)	67.2 (2.9)	84.2 (0.1)	22.39 (0.71)	62.7 (2.0)

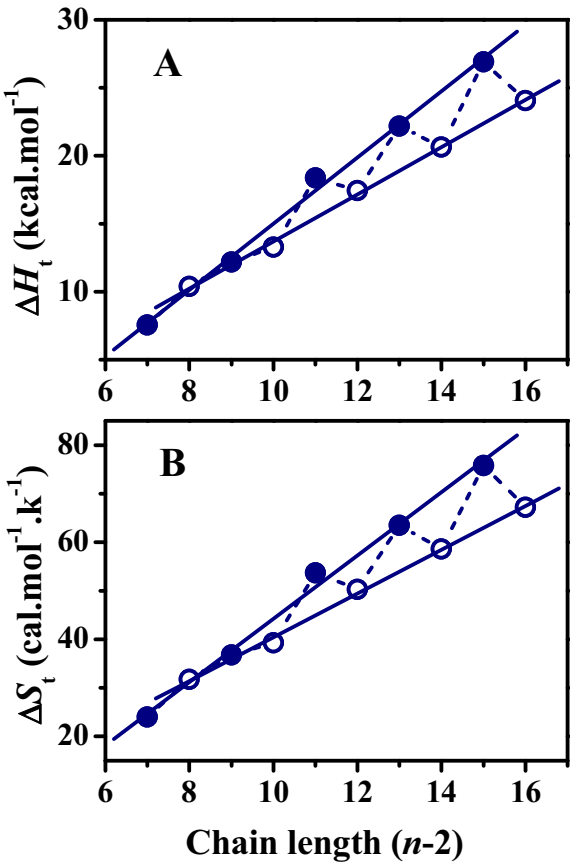

Figure 3. Chainlength dependence of transition enthalpy (A) and transition entropy (B) of dry DAAOHs from the first heating scans. Values of ΔH_t and ΔS_t were plotted against the number of methylene units (n-2). Filled symbols, odd chainlength compounds; open symbols, even chainlength compounds. Solid lines correspond to linear least-squares fits of the data.

NAAOHs.[11,15,19] The values of ΔH_t and ΔS_t obtained for odd- and even chainlength DAAOHs independently exhibit linear dependence on the chainlength. In contrast, ΔH_t and ΔS_t of second heating thermograms (Figure S7, SI) show linear dependence for all DAAOHs, except C9 DAAOH. The ΔH_t and ΔS_t values of first and second heating scans could be fit well to expressions (3) and (4).

$$\Delta H_t = \Delta H_o + (n-2)\Delta H_{inc} \quad (3)$$

$$\Delta S_t = \Delta S_o + (n-2)\Delta S_{inc} \quad (4)$$

Similar linear dependence of the transition enthalpies and entropies was observed previously in several single- and double-chain amphiphiles such as NAAEs, NAAOHs, NAGEs, DAEs, and NAAs.[11–15,19,24] The linear fits yielded incremental values of transition enthalpy and transition entropy (ΔH_{inc}, ΔS_{inc}) from polymethylene groups, and end contributions (ΔH_o, ΔS_o) arising from the terminal methyl group of the acyl chains and the head group. These values obtained from the first and second heating thermograms are given in Table 2.

The linear chainlength dependence of ΔH_t and ΔS_t values, observed here, indicates that molecular packing of the compounds with odd- and even chains would be similar initially (obtained after crystallization from the solvent) within each group, whereas upon going through the melting transition, all DAAOHs (even chain compounds as well as odd chain compounds) might adopt a similar molecular packing. Therefore, molecular packing and intermolecular interactions in the solid-state of all the even-chain

Table 2. Incremental values (H_{inc}, S_{inc}) and end contributions (H_o, S_o) arising from the phase transition enthalpies and entropies of DAAOHs. Values in parentheses correspond to fitting errors obtained from the least-squares analysis.

Thermodynamic parameter	1st Heat		2nd Heat
	Odd chain length	Even chain length	
ΔH_{inc} (kcal/mol)	2.44 (0.09)	1.74 (0.05)	1.55 (0.02)
ΔH_o (kcal/mol)	− 9.36 (1.11)	− 3.66 (0.59)	− 2.35 (0.28)
ΔS_{inc} (cal/mol/k)	6.52 (0.30)	4.50 (0.14)	3.98 (0.05)
ΔS_o (cal/mol/k)	− 20.91 (3.46)	− 4.62 (1.69)	− 0.77 (0.62)

DAAOHs are likely to be somewhat similar (initially), and determination of the 3-dimensional structure of any one of them can give a reasonably good idea of the molecular packing and intermolecular interactions present in the crystal lattice of DAAOHs in the particular series. Interestingly, incremental and end contribution values obtained from second heating thermograms are significantly lower compared to the incremental and end contributions of first heating thermograms (both odd- and even chainlength compounds), which could be due to changes in the molecular packing after the first heating cycle.

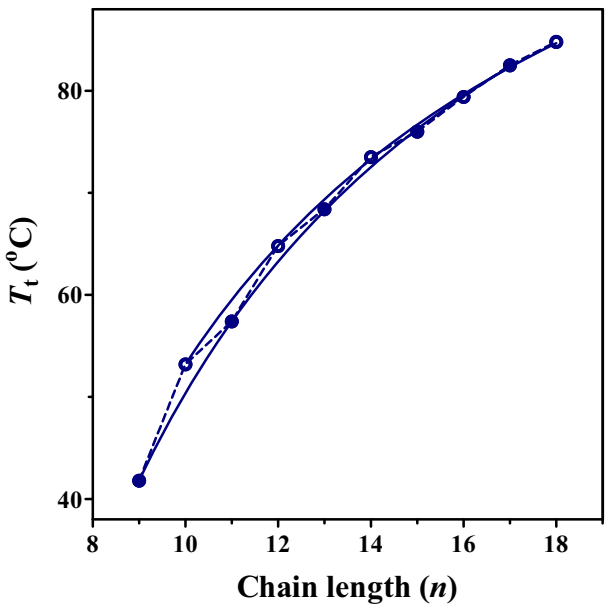

Figure 4. Chainlength dependence of solid-liquid phase transition temperatures (T_t) of DAAOHs. Solid lines correspond to a nonlinear least-squares fit of the transition temperatures to Eq. 8. Filled symbols, odd chainlength compounds; open symbols, even chainlength compounds.

3.3 *Chain length dependence of T_t*

The change in the melting phase transition temperatures (T_t) of DAAOHs in the first heating thermograms is given in Figure 4. The even chainlength DAAOHs have higher T_t values as compared to the odd-chain compounds and within each series, the T_t of DAAOHs increases in a smooth progression with the acyl chainlength, but the differences between the two series decrease with increasing chainlength and after C15 the differences become very small such that the odd-even alternation is not detectable. In general, for many single-chain amphiphiles, T_t values of even chainlength compounds were found to be higher than the odd chainlength compounds,[21,26,27] although some exceptions were reported, e.g., NAAs and L-alanine alkyl esters (AEs).[19,20] The odd-even alternation in the T_t values, enthalpies and entropies in DAAOHs is unusual in that while the even chainlength compounds have higher T_t values, the ΔH_t and ΔS_t values are higher for the odd chainlength compounds. Similar unusual behavior was noticed earlier in AEs.[20]

For compounds with long acyl chains, the end contribution from terminal methyl and the polar head group can be neglected compared to the polymethylene chain portion towards ΔH_t and ΔS_t. Thus, at infinite acyl chainlength, Eqs. (3) and (4) can be reduced to Eqs. (5) and (6), respectively:

$$\Delta H_t = (n-2)\,\Delta H_{inc} \tag{5}$$

$$\Delta S_t = (n-2)\,\Delta S_{inc} \tag{6}$$

Then the T_t for infinite chain length, T_t^{∞}, can be obtained from:

$$T_t^{\infty} = \Delta H_{inc}/\Delta S_{inc} \tag{7}$$

T_t^{∞} values for the NAAOHs have been estimated from the ΔH_{inc} and ΔS_{inc} values presented in Table 2. The

obtained T_t^{∞} for odd- and even chainlength DAAOHs are 101.2 °C (374.2 K) and 113.7 °C (386.7 K), respectively, whereas the T_t^{∞} values obtained for the second heating scans is 116.4 °C (389.4 K).

For many single- and double chain amphiphiles, which show a linear dependence of ΔH_{inc} and ΔS_{inc} on the chain-length, it has been shown that the ΔH_t and ΔS_t values can be fit to the following equation:[28]

$$T_t^{\infty} = \Delta H_t/\Delta S_t = T_t\left[1\left(n_o - n'_o\right)/(n - n_o)\right] \quad (8)$$

where $n_o(= -\Delta H_o/\Delta H_{inc})$ and $n'_o(= -\Delta S_o/\Delta S_{inc})$ are the values of n at which the ΔH_t and ΔS_t are extrapolated to zero. Figure 4 indicates that the T_t values of both odd- and even chainlength DAAOHs obtained from first heating scans fit well to Eq. (8). The T_t^{∞} values obtained for odd- and even chain DAAOHs are 128.9 °C (401.9 K) and 126 °C (399 K), respectively. Similarly, the T_t^{∞} values obtained for odd- and even-chain DAAOHs from second heating thermograms are 130.6 °C (403.6 K) and 122.2 °C (395.2 K), respectively. The T_t^{∞} values obtained for both first and second heating scans of DAAOHs from fitting to Eq. (8) are in good agreement with the T_t^{∞} values estimated using Eq. (7).

3.4 *Comparison of thermodynamic properties of DAAOHs with other diacyl compounds*

It is instructive to compare the thermodynamic parameters associated with the phase transitions of DAAOHs with isomeric NAAEs, as well as with those of homologous DAEs and their isomers, namely the NAGEs. The ΔH_t values of isomeric pair DAAOHs and NAAEs are shown in Figure 5A, and those of the other isomeric pair, namely NAGEs and DAEs are given in Figure 5B. As can be seen from this figure, ΔH_t values of DAAOHs and DAEs are low as compared to the isomeric NAAEs and NAGEs, respectively (although minor differences are observed in even chainlength DAEs at higher chainlength). This indicates that the functional group position plays a key role in the phase transition properties between the isomeric compounds. The ΔH_t values show clear distinction among the four series at lower chainlength. However, the distinction is reduced at higher chainlength due to partial overlap. This complex nature can be understood by comparing their incremental values (ΔH_{inc}) and end contributions (ΔH_o) given in Table 3. If the partial overlap at higher chainlengths is ignored, the ΔH_t values of four series follows the order: NAGEs

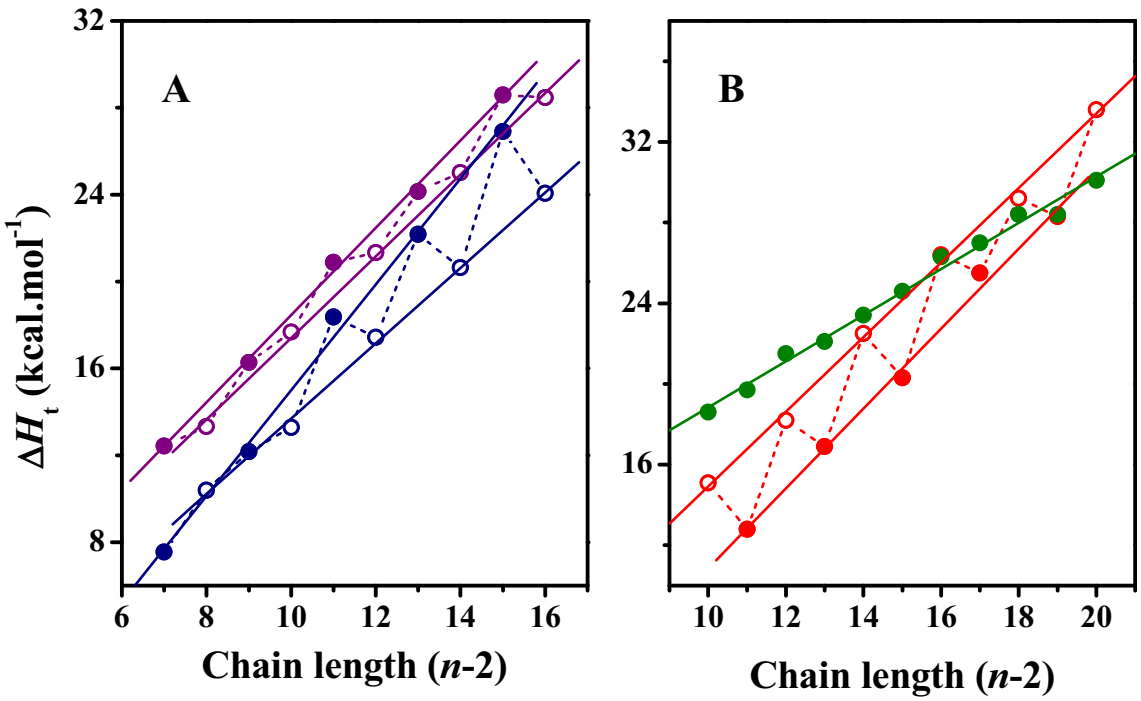

Figure 5. Chain length dependence of transition enthalpies. (**A**) NAAEs (●) and DAAOHs (●). (**B**) NAGEs (●) and DAEs (●). Filled circles, odd chainlength compounds; open circles, even chainlength compounds. Values of ΔH_t were plotted against the number of CH_2 groups in the acyl chains (n-2). Solid lines correspond to linear least-squares fits of the data. For more details, see the text.

Table 3. Incremental values of transition enthalpies (ΔH_{inc}), end contribution (ΔH_o), and transition temperature at infinite chainlength (T_t^{∞}) for NAGEs, DAEs, NAAEs, and DAAOHs.

Lipid	ΔH_{inc} (kcal/mol)	ΔH_o (kcal/mol)	T_t^{∞} (K) Eq. 7	T_t^{∞} (K) Eq. 8	References
NAGEs	1.19 (0.03)	10.16 (0.38)	442.4	409.8	[13]
DAEs (even chainlength)	1.84 (0.04)	0.13 (0.66)	402.6	407.2	[14]
DAEs (odd chainlength)	1.98 (0.09)	− 4.98 (1.19)	396.0	407.2	[14]
NAAEs (odd chainlength)	2.01 (0.05)	− 1.64 (0.59)	400.4	404.8	[11]
NAAEs (even chainlength)	1.88 (0.05)	− 1.39 (0.57)	406.9	402	[11]
DAAOHs (odd chainlength)	2.44 (0.09)	− 9.36 (1.11)	374.2	401.9	Present study
DAAOHs (even chainlength)	1.74 (0.05)	− 3.66 (0.59)	386.7	399	Present study

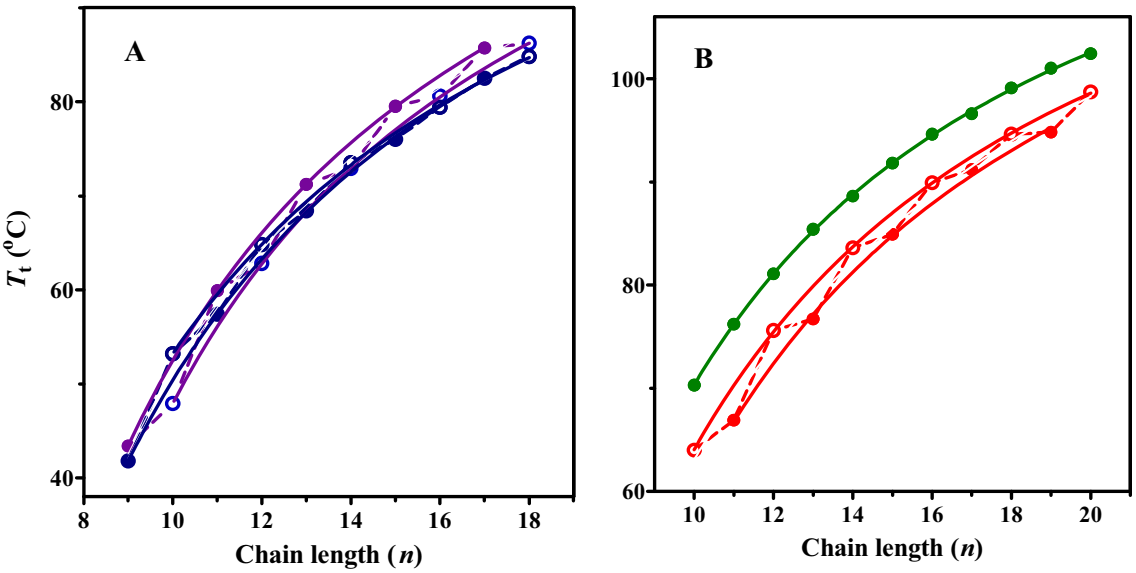

Figure 6. Chainlength dependence of transition temperatures, T_t of different two-chain amphiphiles. (**A**) NAAEs (●) and DAAOHs (●). (**B**) NAGEs (●) and DAEs (●). Filled symbols, odd chainlength compounds; open symbols, even chainlength compounds. Solid lines correspond to nonlinear least-squares fits of the data. For more details, see the text.

> $DAEs_{even}$ = $NAAEs_{odd}$ > $NAAEs_{even}$ > $DAAOHs_{odd}$ > $DAEs_{odd}$ > $DAAOHs_{even}$.

Similarly, a comparison of T_t values of the four series is shown in Figure 6. Chainlength dependence of T_t values of isomeric NAAEs and DAAOHs is shown in Figure 6A, whereas the corresponding plots of NAGEs and DAEs are given in Figure 6B. Similar to the transition enthalpies, the transition temperatures of NAGEs and NAAEs are higher compared to isomeric DAEs and DAAOHs. The difference in T_t values is more distinct at all chainlengths between NAGEs and DAEs, but less so between NAAEs and DAAOHs. The T_t values of the four series are in the following order: NAGEs > $DAEs_{even}$ > $DAEs_{odd}$ > $NAAEs_{odd}$ > $DAAOHs_{even}$ ~ $NAAEs_{even}$ ~ $DAAOHs_{odd}$. The noticed differences could be due to the differential contributions arising from polyethylene chains and end contributions. The T_t^{∞} calculated from Equations 7 and 8 are given in Table 3. Although the T_t^{∞} values obtained show good agreement with the order mentioned above, few differences are observed in case of $DAEs_{odd}$ (Eq. 7) and $DAAOHs_{odd}$ (Eq. 8). These exceptions can be rationalized in terms of molecular packing and intermolecular interactions if crystal structures of several compounds (of both odd and even chainlengths) are determined from each series.

Further, odd-even alternation in ΔH_t (as well as ΔS_t and T_t) of homologous series of single and double chain lipids was explained by differences in the packing of terminal methyl groups of odd- and even chainlength compounds.[27] If the hydrocarbon chains are aligned perpendicular to the plane of the terminal methyl groups, such alteration is not observed. On the

other hand, if the acyl/alkyl chains are tilted with respect to the plane of the terminal methyl groups, the packing is different for the odd- and even-chain compounds and thus leads to changes in the physical properties. This can be seen in Table 3, where the end contribution (ΔH_o) is much different for the four series. Although incremental values of NAGEs are low as compared to isomeric DAEs, due to the significant contribution of terminal methyl groups and the central polar moiety of NAGEs (0-1° tilt angle, untilted bilayer packing), NAGEs have shown higher ΔH_t than isomeric DAEs (32-33° tilt angle, tilted bilayer packing).[13,14] Similarly, though incremental values of NAAEs and DAAOHs are comparable, due to lesser end contributions in DAAOHs, NAAEs have higher ΔH_t than isomeric DAAOHs.

3.5 *PXRD and molecular packing*

Since we could not obtain crystals of DAAOHs that are suitable for single-crystal X-ray diffraction studies, we carried out PXRD studies to derive structural information on these compounds. The PXRD data obtained for odd- and even-chain DAAOHs are shown in Figures 7A and B, except for the C9 compound. All the other DAAOHs (C10−C18) gave several sharp diffraction peaks in the 2θ range of 1−30°. From the diffraction peak positions, the average *d*-spacings were calculated using 3−4 peaks for each DAAOH. The average *d*-spacings obtained are given in Table S5 (SI), and the chainlength dependence of the *d*-spacing is shown in Figure 7C. The *d*-spacing data exhibit a linear dependence on the chainlength, independently for the even- and odd acyl chainlength series with slopes of 0.82 and 0.79Å/CH_2, respectively. The C11 compound which is an outlier was omitted from the fit of the odd chainlength series. Since the estimated increment in the *d*-spacing for each C−C bond in an untilted chain is 1.27 Å/CH_2, the smaller incremental values obtained for DAAOHs suggest that the acyl chains are tilted with respect to the bilayer normal. The value of 0.82 Å for an increase in *d*-spacing per CH_2 for DAAOH is lower than the value of 0.88 Å/CH_2 obtained for the isomeric NAAEs,[11] and suggests that the acyl chains in DAAOHs are more tilted as compared to the chains in NAAEs. While NAGEs are packed in a normal, untilted bilayer packing with the *d*-spacing increment of 1.28 Å/CH_2,[13] the isomeric DAEs are packed in a tilted bilayer.[14] Similar to

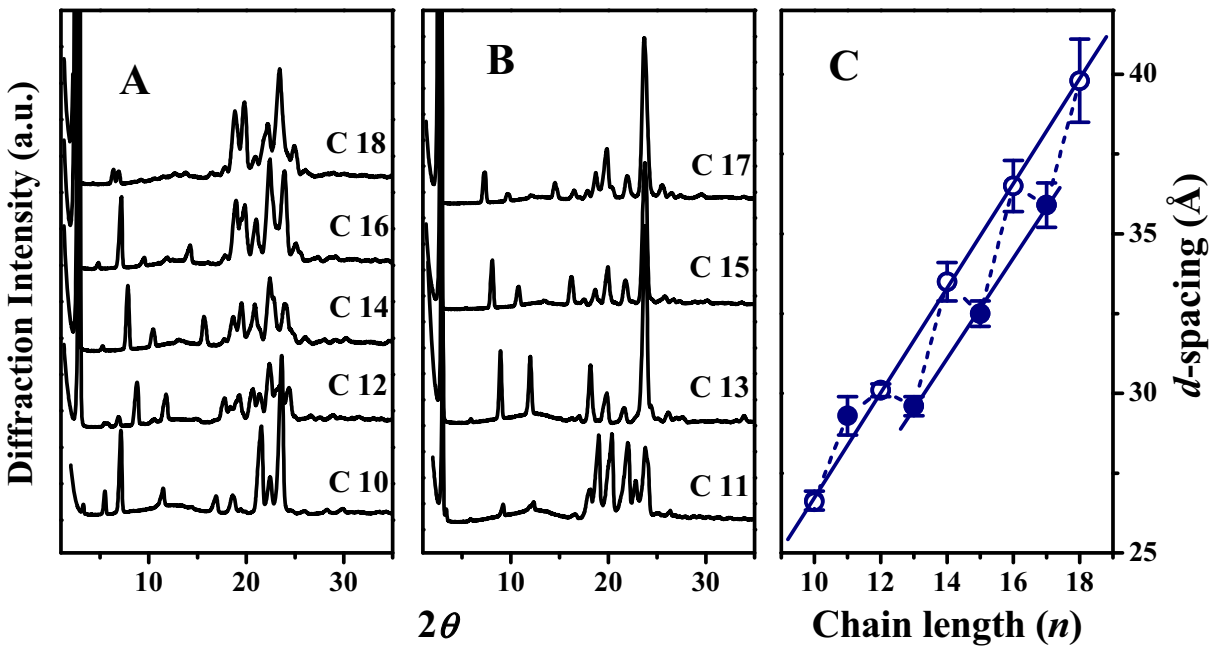

Figure 7. Powder X-ray diffraction patterns of DAAOHs with different saturated acyl chains (**A**, **B**) and dependence of *d*-spacings on the chain length (**C**). The number of C-atoms in the acyl chain is indicated against each PXRD profile. Filled symbols, odd chainlength compounds; open symbols, even chainlength compounds. The solid lines in C represent linear least-squares fit of the data. Data corresponding to C11 compound was omitted from the linear fit as it is an outlier.

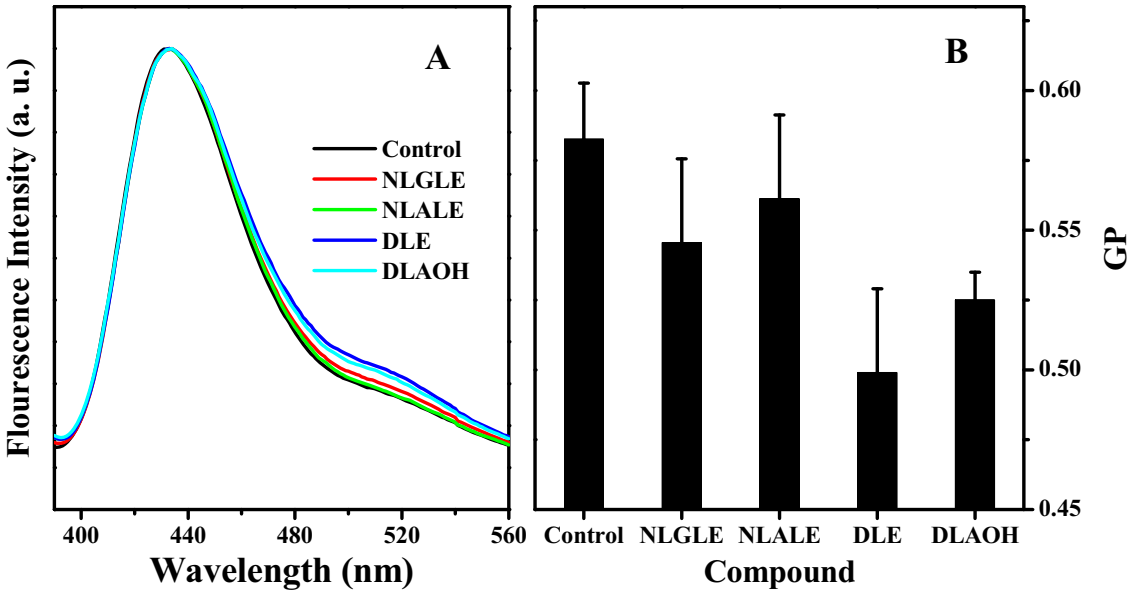

Figure 8. (**A**) Emission spectra of Laurdan in stratum corneum model (SCM) lipid mixture and SCM containing 20 mol% NLGLE, NLALE, DLE, or DLAOH. (**B**) Comparison of Laurdan GP values for the different samples. See text for details.

DAAOHs, DAEs, and NAAEs, dimyristoylphosphatidylglycerol (DMPG) and cerebroside also have tilted bilayer packing.[29,30]

3.6 *Laurdan GP studies on stratum corneum model membranes*

To monitor the change in fluidity, we determined the generalized polarization (GP) of Laurdan for SCM lipid mixture and SCM lipid mixtures to which 20 mol% of DLAOH, DLE, NLALE, or NLGLE was added, which results in 16.7% mol% of the added lipid while the relative proportion of the SCM lipids remains constant. Laurdan is a phase-sensitive dye and shows distinct emission maxima in the gel phase (430-440 nm) and fluid phase (>470 nm).[18] Since the decrease in GP indicates increase in fluidity, which can be correlated to the permeability of the membrane. In the present case, SCM and SCM containing DLAOH, DLE, NLALE, or NLGLE have shown emission maximum at 433 nm (Figure 8A). Upon addition of any of these to the SCM lipid mixture, we noticed a small to moderate decrease in emission intensity at ~490 nm in both cases. Values of laurdan GP calculated from the fluorescence spectral data using eq. 2 are shown in Figure 8B. The results presented in Figs. 8A and 8B reveal that the SCM fluidity is lower for membranes containing DLE and DLAOH compared to isomeric NLGLE and NLALE, respectively. Although, as discussed above, the general trends in the physical properties of these four classes of compounds are broadly similar, the present results on their interaction with stratum corneum model membranes suggest that they may exhibit important differences in their specific interaction with other membrane lipids, which in turn modulate the membrane fluidity. Importantly, these results also indicate that membranes containing *N*, *O*-diacylethanolamines (DAEs) and *N*, *O*-diacyl-L-alaninols (DAAOHs) exhibit higher potential as chemical enhancers for increasing the permeability of SC membranes.

4. Conclusions

In the present work, we report the synthesis and characterization of a homologous series of *N*-, *O*-diacyl alaninols (DAAOHs) of matched acyl chains (n = 9–18). Similar to isomeric NAAEs, DAAOHs displayed an unusual odd-even alternation in transition enthalpies and entropies, with the odd-chainlength compounds exhibiting higher values than the even-chainlength ones. Odd-even alternation was also observed in the transition temperatures of DAAOHs, with the odd-chainlength compounds exhibiting higher values. Powder XRD studies revealed that DAAOHs adopt tilted bilayer packing, which is similar to the isomeric NAAEs. However, DAAOHs were more tilted than NAAEs. Incorporation of *N*, *O*-dilauroylethanolamine (DLE) and *N*, *O*-dilauroyl-L-alaninol (DLAOH) into stratum corneum model membranes decreased the membrane fluidity more than that observed with NAGE and NAAE with

lauroyl chains, suggesting that DAEs and DAAOHs would be better candidates than NAGEs and NAAEs as chemical enhancers in the design of transdermal drug delivery systems. However, further evaluation by permeability studies is required in order to verify this possibility, which will be taken up in our future studies.

Supplementary Information (SI)

Representative FTIR, ^{1}H-NMR, ^{13}C-NMR, and HRMS spectra of *N*, *O*-dilauroyl-L-alaninol (DLAOH) are given in Figures S1–S4. Corresponding spectral data for all DAAOHs (n = 9-18) are given in Tables S1–S4. DSC thermograms for the first cooling scan and second heating scan are given in Figure S5 and S6, respectively. Chain-length dependence of transition enthalpies and entropies are given in Figure S7, and chainlength dependence of transition temperatures from second heating thermograms is given in Figure S8. Supplementary Information is available online at www.ias.ac.in/chemsci.

Acknowledgments

This work was supported by a research Grant from the DST (India) to MJS. DS was supported by a Senior Research Fellowship from the CSIR (India). SKC acknowledges a non-NET fellowship from University Grants Commission (UGC) (India). UGC is acknowledged for their support through the UPE and CAS programs to the University of Hyderabad and School of Chemistry. University of Hyderabad is an Institution of Eminence of the UGC (India).

Declaration

Conflict of interest The authors declare no conflict of interest for this work.

References

1. Kailash V, Pratibha C, Mahavir G, Ashwini P and Mangesh K 2013 Transdermal delivery: A recent trend in treatment of chronic diseases *BioMedRx* **1** 473
2. Meer S, Tahir M A and Abbasi M S A 2020 Formulation-based technology advancements in transdermal drug delivery system *Asian J. Res. Derm. Sci.* **3** 20
3. Elias P M 1983 Epidermal lipids, barrier function, and desquamation *J. Invest. Dermatol.* **80** 44s
4. Sahle F F, Gabre-Mariam T, Dobner B, Wohlrab J and Neubert R H H 2015 Skin diseases associated with the depletion of stratum corneum lipids and stratum corneum lipid substitution therapy *Skin Pharmacol. Physiol.* **28** 42
5. Bonte F, Pinguet P, Chevalier J M and Meybeck A 1995 Analysis of all stratum corneum lipids by automated multiple development high-performance thin-layer chromatography *J. Chromatogr.* **664** 311
6. Holleran W H, Takagi Y and Uchida Y 2006 Epidermal sphingolipids: Metabolism, function, and roles in skin disorders *FEBS Lett.* **580** 5456
7. Haque T and Talukder M M U 2018 Chemical enhancer: A simplistic way to modulate barrier function of the stratum corneum *Adv. Pharm. Bull.* **8** 162
8. Pham Q D, Bjorklund S, Engblom J, Topgaard D and Sparr E 2016 Chemical penetration enhancers in stratum corneum—Relation between molecular effects and barrier function *J. Control. Rel.* **232** 175
9. Karande P and Mitragotri S 2009 Enhancement of transdermal drug delivery via synergistic action of chemicals *Biochim. Biophys. Acta* **1788** 2362
10. Vavrova K, Hrabalek A, Dolezal P, Holas T and Zbytovska J 2003 L-serine and glycine based ceramide analogs as transdermal permeation enhancers: Polar head size and hydrogen bonding *Bioorg. Med. Chem. Lett.* **13** 2351
11. Sivaramakrishna D and Swamy M J 2015 Differential scanning calorimetric and powder X-ray diffraction studies on a homologous series of *N*-acyl-L-alanine esters with matched chains (n = 9–18) *J. Chem. Sci.* **127** 1627
12. Lande M B, Donovan J M and Zeidel M L 1995 The relationship between membrane fluidity and permeabilities to water, solutes, ammonia, and protons *J. Gen. Physiol.* **106** 67
13. Reddy S T and Swamy M J 2017 Molecular structure, supramolecular organization, and thermotropic phase behavior of *N*-acylglycine alkyl esters with matched acyl and alkyl chains *Chem. Phys. Lipid.* **208** 43
14. Kamlekar R K, Tarafdar P K and Swamy M J 2010 Synthesis, calorimetric studies and crystal structures of N, O-diacylethanolamines with matched chains *J. Lipid. Res.* **51** 42
15. Sivaramakrishna D and Swamy M J 2016 Synthesis, characterization and thermotropic phase behavior of a homologous series of N-acyl-L-alaninols and interaction of N-myristoyl L-alaninol with dimyristoylphosphatidylcholine *Chem. Phys. Lipid.* **196** 5
16. Marsh D 1990 *Handbook of Lipid Bilayers* (Boca Raton, FL: CRC Press)
17. Sivaramakrishna D, Prasad M D and Swamy M J A 2019 homologous series of apoptosis-inducing N-acylserinols: Thermotropic phase behavior, interaction with cholesterol and characterization of cationic N-myristoylserinol-cholesterol-CTAB niosomes *Biochim. Biophys. Acta* **1861** 504
18. Parasassi T, Krasnowska E K, Bagatolli L and Gratton E 1998 Laurdan and Prodan as polarity-sensitive fluorescent membrane probes *J. Fluoresc.* **8** 375
19. Sivaramakrishna D, Reddy S T, Nagaraju T and Swamy M J 2015 Self-assembly, supramolecular organization, and phase transitions of a homologous series of *N*-acyl-L-alanines (n = 8–20) *Colloid Surf. A: Physicochem. Eng. Asp.* **47** 108
20. Sivaramakrishna D and Swamy M J 2015 Self-assembly, supramolecular organization and phase behavior of L-alanine alkyl esters (n = 9-18) and characterization of equimolar L-alanine lauryl ester/Lauryl sulphate catanionic complex *Langmuir* **31** 9546

21. Ramakrishnan M and Swamy M J 1998 Differential scanning calorimetric studies on the thermotropic phase transitions of N-acylethanolamines of odd chain lengths *Chem. Phys. Lipids* **94** 43
22. Kamlekar RK and Swamy M J 2006 Molecular packing and intermolecular interactions in two structural polymorphs of N-palmitoylethanolamide, a type 2 cannabinoid receptor agonist *J. Lipid Res.* **47** 1424
23. Reddy S T, Krovi K P and Swamy M J 2014 Structure and thermotropic phase behavior of a homologous series of N-acylglycines: Neuroactive and antinociceptive constituents of biomembranes *Cryst. Growth Des.* **14** 4944
24. Tarafdar P K, Reddy S T and Swamy M J 2012 Nonclassical odd-even alternation in mixed chain diacylethanolamines: Implications of polymorphism *Cryst. Growth. Des.* **12** 1132
25. Sivaramakrishna D and Swamy M J 2016 Structure, supramolecular organization and phase behavior of *N*-Acyl-β-Alanines: Structural homologs of mammalian brain constituents N-acylglycine and N-acyl-GABA *Chem. Phys. Lipid.* **201** 1
26. Reddy ST, Tarafdar PK, Kamlekar RK and Swamy MJ 2013 Structure and thermotropic phase behavior of a homologous series of bioactive *N*-acyldopamines *J. Phys. Chem. B* **117** 8747
27. Larsson K 1986 Physical properties–structural and physical characteristics In *The Lipid Handbook* F D Gunstone, J L Harwood and F B Padley (Eds.) (London: Chapman and Hall) pp. 321–384
28. Marsh D 1982 Biomembranes. In: *Supramolecular Structure and Function* G Pifat and J N Herak (Eds.) (New York: Plenum Press) pp. 127–178
29. Pascher I, Sundell S, Harlos K and Eibl H 1987 Conformation and packing properties of membrane lipids: The crystal structure of sodium dimyristoylphosphatidylglycerol *Biochim. Biophys. Acta* **896** 77
30. Pascher I and Sundell S 1977 Molecular arrangements in sphingolipids. The crystal structure of the cerebroside *Chem. Phys. Lipid.* **20** 175